Interfacial Tension in Binary Polymer Blends in the Presence of Block Copolymers: Effects of Additive MW

H. Retsos, I. Margiolaki, A. Messaritaki, and S. H. Anastasiadis*

Foundation for Research and Technology−Hellas, Institute of Electronic Structure and Laser, P.O. Box 1527, 711 10 Heraklion, Crete, Greece, and University of Crete, Physics Department, 710 03 Heraklion, Crete, Greece

Received December 11, 2000; Revised Manuscript Received March 29, 2001

ABSTRACT: The effect of block copolymer addition on the reduction of the interfacial tension between two immiscible homopolymers is investigated as a function of the additive molecular weight and concentration for polystyrene/polyisoprene blends in the presence of polystyrene-*block*-polyisoprene copolymers using the pendant drop method. The interfacial tension decreases with the addition of small amounts of copolymer and reaches a plateau at higher copolymer concentration, in agreement with previous studies. However, the reduction of the interfacial tension is a nonmonotonic function of the copolymer additive molecular weight at constant copolymer concentration in the plateau region. As the additive molecular weight increases the interfacial tension reduction, $|\Delta\gamma|$, goes through a maximum. This should be related with the increased tendency of micelle formation for high copolymer molecular weights, which is verified by small-angle X-ray scattering. The results are discussed in relation to theoretical predictions for polymer/polymer/copolymer mixtures.

I. Introduction

Improvement of the performance of polymeric materials for many important industrial applications is achieved by mixing two or more components with complementary properties. For the case of immiscible polymer−polymer dispersions, one is faced with the problem of controlling the morphology (phase structure) and the interfacial adhesion between the phases in order to obtain an optimized product. The phase structure (e.g., the dispersed particle size) as well as the equilibrium adhesive-bond-strength between the two phases is related to the interfacial energy and interfacial thickness between the domains.

Suitably chosen block or graft copolymers are widely used by the polymer industry as emulsifiers in multiconstituent polymeric systems.[1,2] This is due to their interfacial activity, i.e., to their affinity to selectively segregate to the interface[2−7] between the phase-separated homopolymers. This partitioning of the block copolymers at the interface is responsible for the significant reduction of the interfacial tension between the two macrophases,[8−12] that leads to a finer and more homogeneous dispersion during mixing,[13−16] provides a measure of stability against gross segregation[14] by inhibiting coalescence[14b] of the dispersed phases, and leads to improved interfacial adhesion[17] and mechanical properties[13,18] via the significant increase[6,19] of the interfacial thickness between the two macrophases. The segments of these compatibilizers can be chemically identical with those in the respective phases[2−20] or miscible with or adhered to one of the phases.[21]

For the block or graft copolymers to be effective, they must partition to the blend interface,[2−7] with each block preferentially extending into its respective homopolymer phase.[6,7,22−25] Since block and graft copolymers are likely to be expensive, it is of great importance to maximize their efficiency, so that only small amounts are required. The tendency of the copolymeric additives to migrate to the interface has been anticipated to depend on the interaction parameter balance between the homopolymers and the copolymer blocks,[26] on the macromolecular architecture/topology and composition of the copolymers,[27] and, very importantly, on the molecular weights of the copolymer blocks[25,28−31] relative to those of the homopolymers. One should always keep in mind, however, that, in a typical preparation of homopolymer/copolymer blends, the system may be diffusion-controlled and the optimal conditions for the molecular design of interfacially active copolymers obtained from equilibrium considerations should be modified. Besides, trapping of high copolymer concentrations at the interface can be envisioned.[22] Moreover, mixing the additive with one on the components may lead to the formation of copolymeric micelles in the homopolymer matrix;[32] the micelles would compete with the interfacial region for copolymer chains and the amount of copolymer at the interface or in micelles would depend on the relative reduction in the free energy. The effect of the existence of micelles on the interfacial partitioning of diblock copolymers at the polymer/polymer interface has not been examined to a significant extent.[3,29,31,33,34]

In this report, the effect of the molecular weight (MW) and concentration (ϕ_{add}) of compositionally symmetric diblock copolymer additives on the interfacial tension between two immiscible homopolymers is investigated, using a technique based on the analysis of axisymmetric pendant fluid drop profiles.[9,10,12,35] The system investigated is polystyrene/polyisoprene blends in the presence of polystyrene-*block*-polyisoprene copolymers. A decrease in interfacial tension is observed with addition of small amounts of copolymer followed by a leveling off (plateau) as the copolymer concentration increases, in agreement with earlier investigations.[8−12] The reduction of the interfacial tension, however, is a nonmonotonic function of the copolymer MW at constant copolymer concentration ϕ_{add} in the plateau regime. For low additive MW's, the interfacial tension reduction in-

* To whom correspondence should be addressed at the Foundation for Research and Technology−Hellas.

10.1021/ma002105s CCC: $20.00
Published on Web 06/19/2001

Table 1. Molecular Characteristics of the Poly(styrene-*b*-isoprene) Samples

code	M_w	M_w/M_n	w_{PS}[a]	N[b]	f_{PS}[c]	previous name	ref
D-1	12 400	1.05	0.44	140	0.41	SI-140	37
D-2	23 300	1.04	0.50	277	0.47	SI(12−12)	38
D-3	36 000	1.05	0.44	432	0.41	SI(16−20)	39
D-4	57 500	1.05	0.56	679	0.53	JG-4	40
D-5	96 000	1.08	0.62	1127	0.59	JG-1	40
D-6	108 200	1.05	0.52	1290	0.49		41
D-7	140 500	1.08	0.41	1694	0.38	JG-2	40
D-8	159 000	1.05	0.57	1876	0.54	SI-57	42
D-9	172 000	1.03	0.53	2042	0.50	SI-53	42
PS	9860	1.05	1.00	112	1.00		
PI	4000	1.06	0.00	81	0.00		41

[a] Polystyrene weight fraction. [b] Based on average segmental volume. [c] Polystyrene volume fraction

creases as the additive MW increases whereas, for even higher MW's, this trend is reversed and the interfacial tension reduction decreases. An attempt to understand this is made by considering the thermodynamic equilibrium among copolymer chains adsorbed at the interface, homogeneously distributed in the bulk homopolymers, and at micelles formed within the homopolymer phases. At low MW's, the equilibrium is between copolymer chains at the interface and chains homogeneously distributed in the bulk (regime I); increasing the MW drives more copolymer chains to the interface, thus decreasing the interfacial tension. However, when micelles are present (regime II), further increase of the MW drives less copolymer to the interface; thus, the interfacial tension reduction is smaller. These ideas are further supported by small-angle X-ray scattering showing the formation of micelles for copolymer MW's in the regime II and their absence in regime I. It is noted that the effect of the macromolecular architecture and the copolymer composition will be reported in a subsequent publication.[36]

The remaining of this article is arranged as follows: Following the Experimental Section, section II, the results of the interfacial tension investigations are presented in section III and are discussed in relation to a theoretical attempt to predict the behavior. The concluding remarks constitute section IV.

II. Experimental Section

Materials. Polystyrene-*block*-poly(1,4-isoprene), SI, diblock copolymer samples were synthesized by anionic polymerization using high vacuum or inert-atmosphere techniques. The characteristics of the diblocks are shown in Table 1 whereas the details of their synthesis and characterization have been described earlier in the respective references of Table 1. It is noted that in the present study the diblocks utilized are more-or-less symmetric in composition.

Polystyrene (PS) homopolymer (Polymer Laboratories, Ltd.) was used in this study as received. Polyisoprene (PI) homopolymer was anionically synthesized under argon atmosphere by J. W. Mays and K. Hong and was kindly provided to the authors. The characteristics of the PS and PI homopolymers are also shown in Table 1.

Interfacial Tension Measurements. The interfacial tension between the two different phases (with and without the compatibilizer) is measured with the pendant drop method using a technique based on the analysis of axisymmetric fluid drop profiles.[9,10,35] Because of the high viscosities and the viscoelastic character of polymeric materials, equilibrium static techniques, such as drop profile methods, are better suited for measuring surface/interfacial tensions; the pendant/sessile drop method has been proven to be the most versatile in that respect (a comparison between different techniques was recently presented by Xing et al.[43]). The method is based on the principle that the shape of the profile of a drop of one fluid into a matrix of another is governed by a force balance between interfacial tension and gravity forces, which is described by the Bashforth−Adams equation.[44] The shape is controlled by the shape parameter $B = a\sqrt{c} = a[g\Delta\rho/\gamma]^{1/2}$, where a is the radius of curvature at the drop apex, g is the gravitational constant, γ is the interfacial tension, $\Delta\rho$ is the density difference across the interface, and $c = g\Delta\rho/\gamma$.

The pendant drop is formed in a heated cell with temperature control up to 300 °C with accuracy ±1 °C. The optical system includes a motorized zoom lens with highest magnification such that a 1 mm subject at distance 10 cm covers an 11-in. screen of the video monitor. The video image of the drop is digitized by an AT&T Targa frame grabber resident within a microcomputer (the instrument described in ref 35 has been commercialized by Materials Interface Associates). The resulting image is processed using global thresholding and near-neighbor analysis to extract the experimental drop profile. This profile is, then, analyzed with a robust shape comparison algorithm, which utilizes the repeated median concept that reduces the five variable optimization (usually needed for shape comparison) to a single variable search of the shape parameter B (the other parameters can be calculated independently[35]). The interfacial tension, γ, is calculated from the value of the magnification at the best-fit value of B, τ^*, since $\tau^* = 1/\sqrt{c} = [\gamma/(g\Delta\rho)]^{1/2}$.

The copolymers are premixed at certain concentrations with the PS homopolymer in toluene followed by slow evaporation of the solvent. Fluid drops of the mixtures are, then, formed at the tip of a glass capillary tube of a Drummond positive displacement syringe in a fluid matrix of the PI phase, i.e., the copolymer is, essentially, preblended with the dispersed phase in order to control more precisely the amount that can diffuse to the interface and to minimize the distance traveled by the copolymer molecules to reach the polymer/polymer interface.[12b] The same preblending procedure was also adopted before not only for interfacial tension studies[10,11] as well as for the preparation of specimens for transmission electron microscopy experiments.[2,14] For symmetric diblock copolymer additives, it is expected that, at equilibrium, the resulting interfacial tension should be insensitive to whether the additive is preblended with homopolymer A or B or both; to check this expectation, for one of the systems (to be discussed below), the additive was introduced either to PS or to PI or half-and-half to both homopolymers.

Images of each drop formed are digitized every 10 min for long periods of time and the profiles are analyzed. Viscoelastic and interfacial equilibrium is considered to have been attained when the extracted values of the interfacial tension do not change with time.[12b] Caution is always taken to avoid degradation of (especially) the PI for long times at 140 °C, where all the measurements reported herein were taken. The samples are always under inert (nitrogen) atmosphere and in most cases the viscosity of the PI matrix is checked after the end of the measurements.

Figure 1 shows the step-by-step performance of the routine for the analysis of the profile of a typical drop of PS in the matrix of PI at 140 ± 1 °C. Following the digital image processing of the actual pendant drop, the present method for the determination of interfacial tension uses a certain number of points along the drop profile (for example the 41 points shown in Figure 1) which are selected by the routine as the experimental (x_i, z_i) points to be used in the comparison with the calculated profiles. The routine is then performing a one-parameter search along the shape parameter B (Figure 1, parts a−d) where the shape parameter B values are 0.370, 0.543, 0.584, 0.609; Figure 1e shows the best fit obtained for the $B = 0.625$. Utilizing the magnification factor τ^* that corresponds to the optimum B value and knowing the densities of the drop and the matrix phase allows calculation of the interfacial tension γ.

Densities: Literature values were used for the calculation of the densities of PS and PI homopolymers. The density

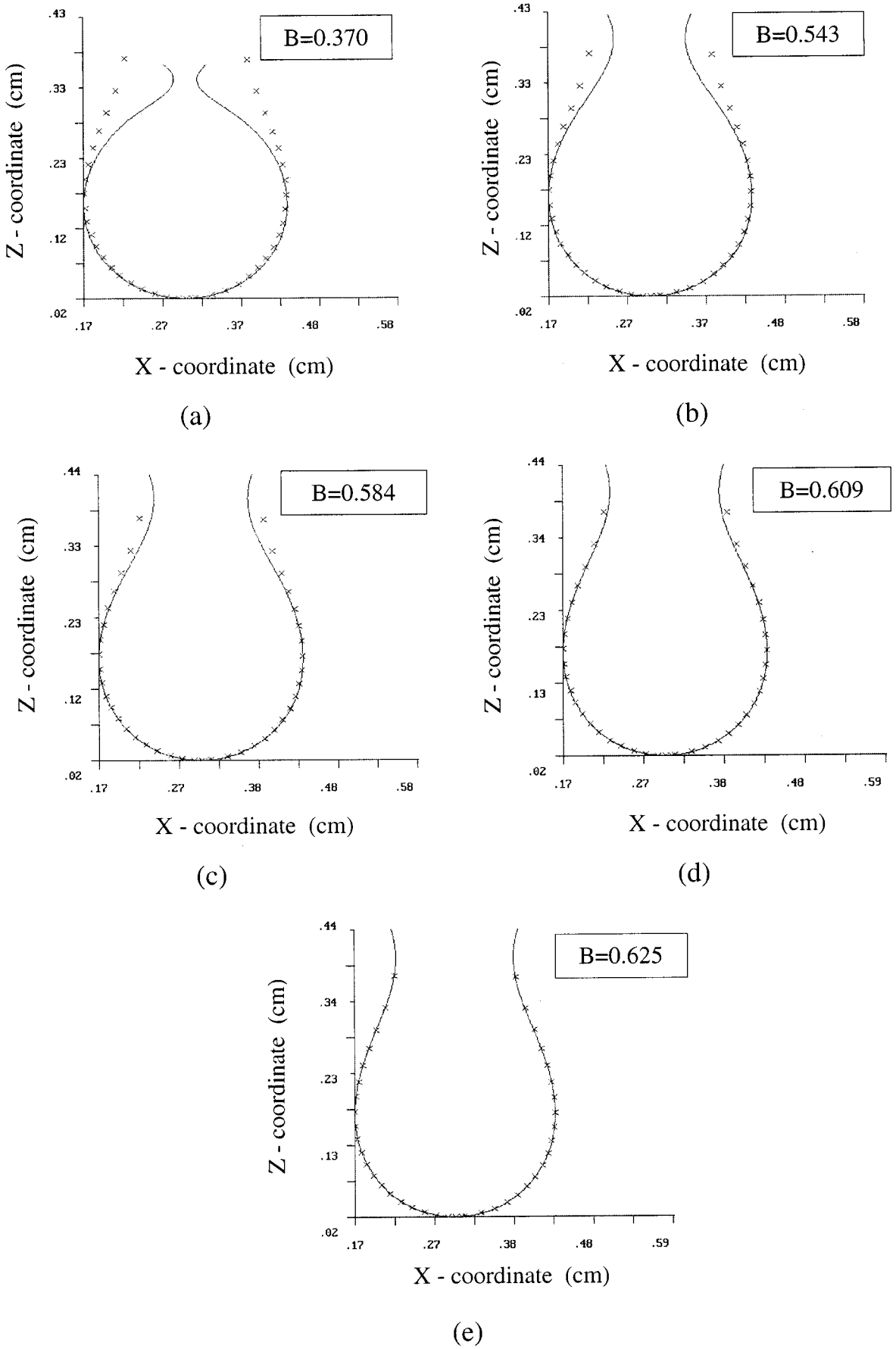

Figure 1. Step-by-step performance of the pendant drop analysis routine: (×) experimental 41 data points selected from the extracted pendant drop profile of a drop of PS in the matrix of PI at 140 ± 1 °C. The lines are the simulated profiles for $B = 0.370$ (a), 0.543 (b), 0.584 (c), and 0.609 (d). The best fit between the experimental profile and the calculated one is obtained for $B = 0.625$ (e).

Table 2. Interfacial Tension at Saturation and Characteristic Concentration w_{char}

copolymer code	γ_{sat} (dyn/cm)	w_{char} (wt %)
D-1	1.60 ± 0.015	*a*
D-2	1.52 ± 0.015	0.39 ± 0.05
D-3	1.48 ± 0.020	*a*
D-4	1.41 ± 0.020	0.31 ± 0.07
D-5	1.31 ± 0.020	0.30 ± 0.05
D-6	1.33 ± 0.020	*a*
D-7	1.40 ± 0.020	*a*
D-8	1.45 ± 0.025	0.39 ± 0.07
D-9	1.63 ± 0.025	*a*

[a] Not enough data points at low concentrations were measured for these copolymers in order to extract values for w_{char}.

of PS is estimated from[45]

$$1/\rho_{PS} = 0.9199 + 5.098 \times 10^{-4}(T - 273) + 2.354 \times 10^{-7}(T - 273)^2 + \frac{32.46 + 0.1017(T - 273)}{M_{w,PS}} \quad (1)$$

where ρ_{PS} is in g/cm^3, T in K, and $M_{w,PS}$ the weight-average molecular weight of PS. The density of PI is similarly estimated from[46]

$$1/\rho_{PI} = 1.0771 + 7.22 \times 10^{-4}(T - 273) + 2.346 \times 10^{-7}(T - 273)^2 \quad (2)$$

where ρ_{PS} is in g/cm^3. Since the weight fractions of copolymers added is always small (less or equal to 4%), it is assumed that the addition does not affect appreciably the density difference across the interface. The maximum possible uncertainty this assumption introduces is less than 2.7% for all the concentrations investigated and less than 1.4% for the 2 wt % concentration; this is well within the error bars of the measurements (see for example Table 2). It should be noted that the accuracy in the extracted values of the interfacial tension is directly proportional to the accuracy in the estimation of the density difference $\Delta\rho$.

Small-Angle X-ray Scattering: Small-angle X-ray scattering (SAXS) experiments were performed on mixtures of polyisoprene with the various polystyrene-*block*-polyisoprene copolymers utilizing a Rigaku 2263A3 camera with slit collimation (slits 0.03 mm at distance 112 mm apart) equipped with an one-dimensional position sensitive detector (straight metal wire). The sample to detector distance is such that scattering wave vectors $q = (4\pi/\lambda) \sin(\theta/2)$ as low as 0.012 Å^{-1} can be measured without interference from the beam stop (θ is the scattering angle and λ is the wavelength of the X-rays). The X-rays were produced by a Rigaku 12 kW rotating anode X-ray generator and the Cu Kα radiation was used ($\lambda = \lambda_{Cu\ K\alpha} = 1.54$ Å). The smeared intensities were collected in a multichannel analyzer and transferred to an HP workstation for further analysis. The data have been corrected for absorption, background scattering, and slit-length smearing. The background correction was made by subtracting from the total intensity the contribution of density fluctuations evaluated from measuring pure PS and pure PI (at the same temperature) and calculating the weighted average based on the composition of the sample in PS and PI. Desmearing was performed (when explicitly stated) using an algorithm by Strobl.[47] In principle, analysis of the SAXS data can be performed following the method outlined by Roe and coworkers[48] for the determination of the micelle characteristics. However, the micelles were too large for the scattering vector range of our SAXS camera and, therefore, it was not possible to extract information on their size.

III. Results and Discussion

Experimental Interfacial Tension Data. Figure 2 shows the interfacial tension data γ for the PS/SI/PI systems as a function of copolymer concentration at a constant temperature of 140 ± 1 °C for four different diblock molecular weights. The copolymer concentration is expressed as weight of the copolymer per weight of the PS. A sharp decrease in the interfacial tension is observed with addition of small amounts of diblock copolymer, once more illustrating the expected surfactant-like behavior of the copolymer. The interfacial tension levels off as the additive concentration increases to a value γ_{sat}; this is usually attributed to interfacial saturation and/or to micelle formation by the copolymer. These observations are in agreement with previous investigations on other systems[8−12] and go along with observations of the behavior of the dispersed phase dimension in heterogeneous blends in the presence of diblock copolymer additives.[15] The concentration dependence can be described with an empirical equation proposed by Tang and Huang[16] and also used by Jorzik and Wolf,[11b] written here in terms of the additive weight fraction w_{add}

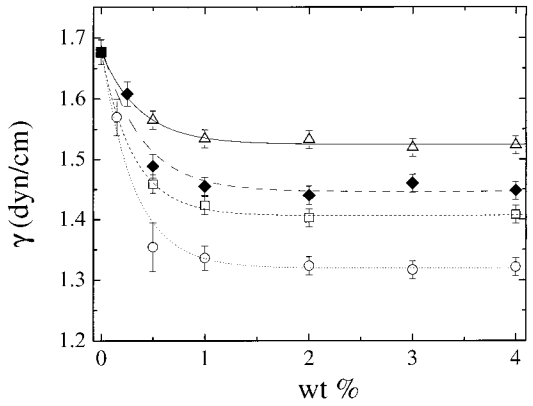

Figure 2. Interfacial tension for the PS/SI/PI systems as a function of copolymer concentration added to the polystyrene phase at a constant temperature of 140 ± 1 °C for four different diblock molecular weights: (△) D-2, (□) D-4, (○) D-5, and (◆) D-8. The lines are fits to eq 4 with the parameters of Table 2 whereas (■) denotes the PS/PI interfacial tension in the absence of the diblock.

$$\gamma = (\gamma_0 - \gamma_{sat}) \exp(-w_{add}/w_{char}) + \gamma_{sat} \quad (3)$$

where γ_0 is the interfacial tension in the absence of copolymer ($\gamma_0 = 1.68 \pm 0.02$ dyn/cm) and w_{char} denotes the concentration required to achieve 1/*e* of the maximum reduction $\gamma_0 - \gamma_{sat}$. Table 2 lists the values of γ_{sat} and w_{char} for the copolymers shown in Figure 2 as well as the values of γ_{sat} for all other systems. Not enough data points at low concentrations were measured for other molecular weights and, therefore, values for w_{char} are not given. The effect of the copolymer MW on w_{char} values is not further discussed anyway since, for all our data, the 1/*e* reduction of interfacial tension happens at very low concentrations in the lower limit of the experimental range investigated.

The aim of the present work is to probe the dependence of the interfacial tension reduction $\gamma_0 - \gamma_{sat}$ on the additive molecular weight (MW). For the lower copolymer MW's of Figure 2, increasing the additive MW enhances the surfactant-like behavior; i.e., γ_{sat} decreases as MW increases. However, with a further increase of the copolymer MW, the value of γ_{sat} increases again as the diblock MW increases. The addition of the higher MW diblock still shows the surfactant behavior expected for diblock copolymers at a polymer/polymer interface

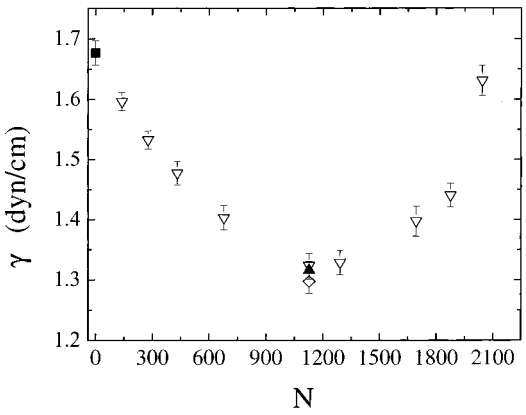

Figure 3. Interfacial tension for the PS/SI/PI systems as a function of the number of segments of the copolymers at a constant temperature of 140 ± 1 °C and constant 2 wt % copolymer added to the polystyrene phase (▽). For the D-5 diblock, data are also shown when 2 wt % copolymer is added to polyisoprene (▲) and when 1 wt % is added to polystyrene and 1 wt % is added to polyisoprene (◊). ■ denotes the PS/PI interfacial tension in the absence of the diblock.

but its efficiency as an emulsifier is reduced relative to lower MW's.

The two opposite trends in Figure 2 are more clearly seen in Figure 3. Here, the interfacial tension data are shown for PS/SI/PI systems with 2 wt % diblock at a constant temperature of 140 ± 1 °C as a function of the total number of segments of the copolymer, N; note that for all systems this concentration corresponds to the plateau value of interfacial tension γ_{sat}. It is noted that the diblock molecular weights used cover the range from about the MW of the homopolymers to about 20 times higher. At low N's, the interfacial tension reduction γ_{sat} increases with increasing N (γ_{sat} decreases), whereas, above a certain additive MW, γ_{sat} decreases by further increasing N (γ_{sat} increases again). The increase of γ_{sat} at high N's is less steep than the decrease at low N's. For copolymer D-5, the interfacial tension data are also shown for the cases where the copolymer was preblended with the PI matrix (at 2 wt %) as well as when it was added as 1 wt % in PS and 1 wt % in PI; the agreement of the three values is evident and is due to the symmetry of the diblocks.

The change of the behavior with copolymer MW can only be understood if the possibility of micelle formation as the diblock MW increases is taken into account. At low N's, the copolymer chains adsorbed at the interface are in equilibrium with copolymer chains which are homogeneously mixed with the bulk homopolymers; increasing the MW should be driving more copolymer chains to the interface thus decreasing the interfacial tension. This situation is the usual assumption made in theoretical treatments,[28−31] which predict a decrease in interfacial tension by increasing the copolymer MW. However, as will be discussed in the next section, when micelles are also considered in the calculation, then, although at low N's the situation is exactly as described above, when the MW increases further and micelles are formed, the copolymer chains at the interface are in equilibrium with copolymers within micelles and with (few) chains which are homogeneously mixed with the homopolymers. In this range of N's, as the MW increases fewer copolymer chains should be driven to the interface, thus reducing the emulsifying effect.

Theoretical Considerations. Statistical thermodynamic theories have been formulated to understand and predict the emulsifying behavior of block copolymers at the polymer/polymer interface.[28−31,49] In a seminal series of papers, Noolandi and co-workers[28] utilized their theory of inhomogeneous systems[50] in order to investigate the polymer density profiles in the interfacial region for a system of two immiscible homopolymers A and B diluted with solvent in the presence of a diblock copolymer A−B. The resulting equations were solved numerically to obtain the segment density profiles and to calculate the interfacial tension under the assumption that the part of the copolymer, which is not localized at the interface, is randomly distributed in the bulk homopolymer phases; therefore, their results should be reliable for low copolymer concentrations below the critical micelle concentration (cmc). Even more, their mean-field theory cannot adequately describe the critical crossover regime from a random copolymer distribution to aggregation (micelle formation), and thus, they only gave a rough estimate of the cmc.

The calculated interfacial density profiles showed greater exclusion of the homopolymers from the interfacial region as the copolymer MW increased; this greater localization of the copolymer resulted in a greater reduction of γ with increasing copolymer MW. Neglecting the conformational entropy of both copolymer and homopolymer chains at the interface (which was found to contribute negligibly to $\Delta\gamma = \gamma_0 - \gamma$) and observing that in their calculations the width-at-half-height of the copolymer profile, d, is independent of the copolymer MW, they approximated the interfacial tension reduction $\Delta\gamma$ as

$$\frac{\Delta\gamma b^2}{k_B T} = \frac{(\gamma_0 - \gamma)b^2}{k_B T} \cong \frac{d}{b}\phi_+\left\{\left(\frac{1}{2}\chi\phi_p + \frac{1}{N}\right) - \frac{1}{N}\exp\left(\frac{N\chi\phi_p}{2}\right)\right\} \quad (4a)$$

where χ is the Flory−Huggins interaction parameter, N is the number of segments of the copolymer, $\phi_+ = \phi(\infty) = \phi(-\infty)$ is the copolymer volume fraction in the bulk homopolymer phases (which is very close to the nominal amount of copolymer present, ϕ_{add}), ϕ_p is the total polymer volume fraction ($\phi_s = 1 - \phi_p$ is that of the solvent present), and b is the statistical segment length. For $N\chi\phi_p \ll 1$, eq 4a reduces to

$$\frac{\Delta\gamma b^2}{k_B T} \cong \frac{d}{b} N\phi_+\chi^2\phi_p^2/8 \quad (4b)$$

Therefore, the theory predicts an exponential dependence of $\Delta\gamma$ on N for large N's and a linear dependence on N and ϕ_+ for small χN's. Noolandi and Hong[28] noted, however, that the interfacial tension surface is bounded by a micellization curve and that their results should be considered reliable only for $N\chi\phi_p \geq 2$.[28b] Noolandi[10,51] has suggested that the theory can be applied to systems without solvent by letting $\phi_p \rightarrow 1$. The data in Figure 2 do not include points in the $N\chi\phi_p \ll 1$ regime and, thus, the scaling of $\Delta\gamma$ on $N\phi_+$ (of eq 4b) is not experimentally observed.[10]

Shull and Kramer[30] developed and applied the Noolandi−Hong theory for the case without solvent. They found that, at a given value of the chemical potential of the copolymer in the bulk phases μ_c, the ability of a copolymer to reduce γ is highest for small N and small χ. However, at a given value of ϕ_+, higher N's result in

a much higher $\Delta\gamma$ due to the exponential dependence of μ_c on χN and since an increase in μ_c results in an increase of the density of copolymer chains at the interface. Theoretical determination of the limiting value of μ_c associated with the formation of micelles was made separately,[3] since the possibility of micelle formation was not explicitly introduced in the theory. A good agreement was found[3] with experimental data for the total amount of copolymer segregating to a polymer−polymer interface for concentrations below cmc using only χ as an adjustable parameter. Using this best-fit value of χ, they estimated $\Delta\gamma$ for concentrations when micelles are not present. For concentrations higher than the cmc, more micelles will be formed without, however, significantly increasing the copolymer chemical potential, thus, the interfacial tension would not decrease further. For the copolymer MW's used, a significant increase of the total copolymer amount adsorbed at the interface was observed at higher copolymer concentrations, which was attributed[3,33] to segregation of micelles to the polymer−polymer interface (as well to the polymer−air surface[3,33,52]). The location of the upturn was used to estimate the copolymer chemical potential at the cmc, which was in good agreement with a full self-consistent-field theoretical estimate.[53]

Semenov[34] presented an analytical mean-field theory for the equilibrium (and dynamics) of block copolymers in a homopolymer layer (between an interface with another homopolymer and the free surface) for high copolymer MW's. The predictions for the total amount of copolymer segregated to the interface are consistent with those of Shull and Kramer[30] for the Shull et al.[3] data. Moreover, Semenov analyzed the situation for concentrations higher than the cmc and found that micelles strongly attract each other thus tending to form a separate micellar macrophase whereas they are also attracted to the free surface and (somewhat weaker) to the interface especially for high copolymer MW's. Moreover, the formation of micelles was found to be an activated process usually with a high barrier and, so, the apparent cmc may be appreciably higher than the equilibrium one. Semenov did not investigate the interfacial tension reduction due to the copolymer segregation to the polymer−polymer interface.

Below an attempt is made to provide a semiquantitative analysis of the interfacial activity of copolymers at the homopolymer interface by modifying the analysis of Leibler.[29] A flat interface is considered with surface area A between phase separated amorphous A and B homopolymers. The thickness of the interfacial region $a_I = b(6\chi)^{-0.5}$ and the interfacial tension $\gamma_0 = k_BTb^{-2}(\chi/6)^{0.5}$ are independent of the number of segments of the two homopolymers[54] (P_A and P_B, respectively) for a highly incompatible situation of $\chi P_i \gg 1$; k_BT is the thermal energy (it is assumed that both types of links have the same segmental volume $v = b^3$). Suppose that Q copolymer chains with $N = N_A + N_B$ segments and composition $f = N_B/N$ are adsorbed at the A/B interface (for most practical situations, $\chi N_i \gg 1$). It is expected that the copolymer joints are localized in a thin interfacial layer of thickness[34] $d' = (\pi/2)a_I$ (independent of N_i and P_i); d' is equal to the semiempirical parameter d of Noolandi et al.[28] in eq 4 as discussed by Semenov.[34] The blocks A and B extend toward the respective bulk layers and form two "adsorbed layers" of thickness L_A and L_B, respectively. Since $d' \ll L_i$, each side of the interfacial film resembles a layer of polymers anchored by one end onto a wall. The free energy of the interfacial film can, thus, be approximated as[29]

$$F_{\text{interf.film}} = \gamma_0 A + Q(g_A + g_B) \tag{5}$$

γ_0 is the A−B interfacial tension in the absence of the additive, A is the interfacial area, and g_A, g_B represent the free energies per chain of the A and B layers. $\sigma = Q/A$ denotes the number of copolymer chains per unit interfacial area.

The majority of the present work concerns the situation where the copolymer chains are not so long relative to the homopolymers. In this case mixing of the N copolymer and P homopolymer chains should be taken into account due to the homopolymers penetrating the chains anchored at the interface whereas the copolymer chains can be either stretched or not. For stretched copolymer chains, this represents the wet brush regime whereas if no stretching is assumed, the copolymer configuration will be that of a wet mushroom. Neglecting the composition gradients in the brush[55] (Flory approximation), g_i has the following main contributions[4,29,56]

$$\frac{g_i}{k_BT} = \ln(N_ib^2\sigma) + L_i\frac{1}{\sigma b^3 P_i}(1-\eta_i)\ln(1-\eta_i) + \frac{3}{2}\frac{{L_i}^2}{N_ib^2} \tag{6}$$

where $\eta_i = \sigma N_i b^3/L_i$ is the average volume fraction of monomers of the i-th block in the layer and $(1-\eta_i)$ is that of the P_i monomers. The first two terms approximate the entropy of mixing between N and P chains, which tend to swell the copolymer blocks; the first term is associated with the translational freedom of the copolymers in the two-dimensional film, whereas the second one originates from the translational entropy of the P chains and has a standard excluded volume form.[56] The last term represents the elastic entropy term, which limits the swelling. For low values of $\eta_i \ll 1$, eq 6 can be written as[4,29]

$$\frac{g_i}{k_BT} = \ln(N_ib^2\sigma) + \frac{1}{2}\frac{N_i\eta_i}{P_i} + \frac{3}{2}\frac{{L_i}^2}{N_ib^2} \tag{7}$$

For stretched chains, the brush thickness L_i and the block monomer concentration η_i are obtained from eq 7 by minimization with respect to L_i. In this case, $L_i = 6^{-1/3}N_ib(\sigma b^2)^{1/3}P_i^{-1/3}$, $\eta_i = 6^{1/3}(\sigma b^2)^{2/3}P_i^{1/3}$, and

$$\frac{g_i}{k_BT} = \ln(N_ib^2\sigma) + \frac{3^{4/3}}{2^{5/3}}(\sigma b^2)^{2/3}\,N_iP_i^{-2/3}\ \text{(wet brush)} \tag{8a}$$

which is valid for $P_iN_i^{-3/2} < \sigma b^2 < P_i^{-1/2}$. For non-stretched chains, $L_i \approx N_i^{1/2}b$ and the last term of eq 7 can be neglected; this applies for[56] $\sigma b^2 < P_iN_i^{-3/2}$. Then, $\eta_i = \sigma b^2 N_i^{1/2}$ and

$$\frac{g_i}{k_BT} = \ln(N_ib^2\sigma) + \frac{1}{2}\frac{N_i^{3/2}\sigma b^2}{P_i}\ \text{(wet mushroom)} \tag{8b}$$

The interfacial tension in the presence of the copolymer is calculated as[57]

$$\gamma = \frac{\partial F_{\text{interf.film}}}{\partial A}|_{Q} = \gamma_0 - \sigma^2\left(\frac{\partial g_A}{\partial \sigma} + \frac{\partial g_B}{\partial \sigma}\right) \quad (9)$$

Therefore, the interfacial tension reduction, $\Delta\gamma = \gamma_0 - \gamma$, is

$$\frac{\Delta\gamma}{k_B T} = \frac{\gamma_0 - \gamma}{k_B T} = \begin{cases} \sigma\left[2 + \frac{3^{1/3}}{2^{2/3}}(\sigma b^2)^{2/3}(N_A P_A^{-2/3} + N_B P_B^{-2/3})\right] \\ \qquad\qquad \text{(wet brush)} \\ \sigma\left[2 + \frac{1}{2}\sigma b^2 (N_A^{3/2} P_A^{-1} + N_B^{3/2} P_B^{-1})\right] \\ \qquad\qquad \text{(wet mushroom)} \end{cases} \quad (10)$$

where the dependence $\Delta\gamma$ on the density of adsorbed chains, σ, is evident.

At equilibrium, σ is determined by equating the chemical potential of the copolymer chains at the interface with that of the copolymer chains either homogeneously mixed with the homopolymers or at micelles formed within the homopolymer phases. The chemical potential of a copolymer chain at the interface is calculated using eq 5 as

$$\mu_{\text{int}} = \frac{\partial F_{\text{interf.film}}}{\partial Q}|_{A} = g_A + g_B + \sigma\left(\frac{\partial g_A}{\partial \sigma} + \frac{\partial g_B}{\partial \sigma}\right) \quad (11)$$

Therefore, with eqs 8

$$\frac{\mu_{\text{int}}}{k_B T} = 2 + \ln(N_A \sigma b^2) + \ln(N_B \sigma b^2) + \begin{cases} 2.271(\sigma b^2)^{2/3}(N_A P_A^{-2/3} + N_B P_B^{-2/3}) \\ \qquad\qquad \text{(wet brush)} \\ \sigma b^2 (N_A^{3/2} P_A^{-1} + N_B^{3/2} P_B^{-1}) \\ \qquad\qquad \text{(wet mushroom)} \end{cases} \quad (12)$$

The free energy density of a homogeneous mixture of an A−B copolymer with an A homopolymer is[34]

$$\frac{F_{\text{bulk}}}{k_B T} = \frac{\phi}{N}\ln\left(\frac{\phi}{e}\right) + \frac{1-\phi}{P_A}\ln\left(\frac{1-\phi}{e}\right) + \chi\phi f(1-f\phi) \quad (13)$$

Thus, the chemical potential of a copolymer chain homogeneously distributed in the bulk, $\mu_{\text{bulk}} = N[(1-\phi)\partial F_{\text{bulk}}/\partial\phi + F_{\text{bulk}}]$, is

$$\frac{\mu_{\text{bulk}}}{k_B T} = \ln\phi - \phi - (1-\phi)\frac{N}{P_A} + \chi f N(1 - 2f\phi + f\phi^2) \quad (14)$$

where $\phi = \phi_+$ is the copolymer volume fraction in the A-rich homopolymer phase.

The chemical potential of a copolymer chain in a micelle was evaluated by Semenov[34] for long homopolymer chains, which do not penetrate the micelles ($P < N$), using his earlier approach[58] for micelles in a copolymer melt. Since, in the present investigation, almost symmetric copolymers are considered, the micelle morphology should be lamellar.[34,59] The free energy of a micelle is, then[34,58]

$$\frac{F_{\text{lam.mic.}}}{k_B T} = Q_{\text{mic}}[0.206x^2 f^{-1} + (\chi f N)^{0.5} x^{-1} + \ln(x/f) + 0.5\ln(\chi f N) - \ln(\pi e/2)] \quad (15)$$

where Q_{mic} is the number of copolymer chains in a micelle, and x is the reduced thickness of the micelle, $x = 0.5 d_{\text{mic}} f^{0.5} R_{g,c}^{-1}$, with d_{mic} its thickness and $R_{g,c} = N^{0.5} b/\sqrt{6}$ the radius of gyration of the copolymer; for lamellar micelles, Q_{mic} is independent of x. After minimization of $F_{\text{lam.mic.}}/Q_{\text{mic}}$ with respect to x, the chemical potential is determined by

$$\mu_{\text{mic}} = \partial F_{\text{lam.mic.}}/\partial Q_{\text{mic}} = F_{\text{lam.mic.}}/Q_{\text{mic}}|_{x=x_{\text{min}}} \quad (16)$$

where x_{min} is the value at the minimum of $F_{\text{lam.mic.}}/Q_{\text{mic}}$. Semenov[34] predicts that, although lamellar micelles are the thermodynamically stable geometry, the high barriers for their formation may lead to the observation of spherical micelles even for symmetric diblocks. For the purposes of our discussion here, however, we present the calculations for the equilibrium lamellar micelle morphology.

For molecular weights and concentrations when micelles are not present, the equilibrium exists between homogeneously distributed copolymer and copolymer at the interface; σ is, then, determined by

$$\mu_{\text{int}}(\sigma;N) = \mu_{\text{bulk}}(\phi_+;\, N) \quad (17a)$$

where, in this case, it is assumed that $\phi = \phi_+ \cong \phi_{\text{add}}$. In the presence of micelles and at thermodynamic equilibrium, σ should be determined by the equation

$$\mu_{\text{int}}(\sigma;N) = \mu_{\text{mic}}(N) = \mu_{\text{bulk}}(\phi_+;\, N) \quad (17b)$$

which also determines the volume fraction ϕ_+ of copolymers remaining homogeneously distributed in the bulk.

For the calculation of the interfacial tension reduction, the chemical potentials μ_{int}, μ_{mic}, and μ_{bulk} are evaluated as a function of σ for $\phi = \phi_+ = \phi_{\text{add}}$. If $\mu_{\text{bulk}}(\phi_{\text{add}}) < \mu_{\text{mic}}$, then the equilibrium exists between copolymers at the interface and copolymers homogeneously mixed in the A-rich phase. The interfacial excess σ is, then, determined by eq 17a together with eqs 12 and 14, and the interfacial tension reduction $\Delta\gamma$ by eq 10. If $\mu_{\text{bulk}}(\phi_{\text{add}}) > \mu_{\text{mic}}$, equilibrium is established among the three different states of the copolymer and σ and ϕ_+ are determined by eq 17b together with eqs 12, 14, and 16; $\Delta\gamma$ is evaluated by eq 10.

Although the assumptions involved do not allow a quantitative comparison, the behavior of $\Delta\gamma$ when the copolymer molecular weight increases at constant additive concentration resembles the experimental data. Figure 4 shows the estimated surface density of copolymers at the A/B interface, σ, together with the interfacial tension reduction $\Delta\gamma = \gamma_0 - \gamma$ as a function of the number of segments of the copolymeric additive for $\phi_{\text{add}} = 0.02$. The parameters used are $P_A = P_{PS} = 112$, $P_B = P_{PI} = 81$, $\chi = 0.04$. Moreover, for the present range of P_i's and N_i's, the wet-mushroom configuration for the adsorbed copolymer chains is assumed (i.e., eqs 12b and 10b are used), which is then verified by the extracted σ values. It is found that the magnitude of the $\Delta\gamma$ increases with copolymer MW as long as the copolymer chains at the interface are at equilibrium with only homogeneously mixed chains and micelles do not exist (regime I). At higher MW's, when micelles are also

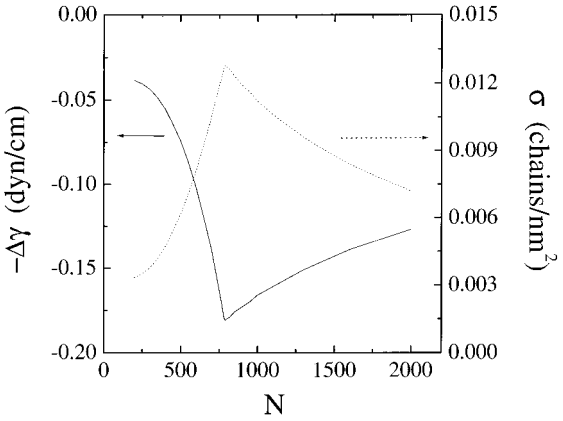

Figure 4. Theoretically estimated interfacial tension reduction, $\Delta\gamma = \gamma_0 - \gamma$ (solid line), and estimated surface density of copolymer chains adsorbed at the interface, σ (dotted line), for the PS/SI/PI systems according to the model presented in the text as a function of the number of segments of the copolymer at constant 2 wt % copolymer concentration and for constant $\chi = 0.04$.

present, $\Delta\gamma$ decreases with further increasing MW (regime II). The values for the $\Delta\gamma$ are in the range of the experimental values although the functional form of the curve is different from the experimental one. For example, the copolymer MW at the minimum is underestimated, indicating that micelles are calculated to form earlier than in the experimental system, whereas the minimum is much sharper than in the experiment; both are related to the functional form used for the free energy of the micelles and the inherent assumptions made therein. The value of the interaction parameter used affects both the location of the minimum (with respect to N) and the values of $\Delta\gamma$; no fitting was attempted since the aim of the theoretical analysis is to obtain only the trends in order to understand the behavior of the experimental data. Indeed, it is evident that the calculation indicates a behavior very similar to the data. The origin of this trend is evidently related to the behavior of the estimated interfacial density of adsorbed chains, σ, also shown in Figure 4. Increasing the copolymer MW when micelles are not present (for the low MW side, regime I) drives rapidly more copolymer chains to the interface (σ increases), thus leading to an increase of $\Delta\gamma$. On the other hand, further increase of the copolymer MW when micelles are present (regime II) leads to a decrease in the surface density of copolymers σ, thus reducing $\Delta\gamma$.

SAXS Measurements. To verify that the absence or the formation of micelles is the reason for the nonmonotonic dependence of γ_{sat} on diblock MW, small-angle X-ray scattering measurements were performed on homopolymer/copolymer mixtures as a function of concentration, molecular weight, and temperature. Figure 5 shows the (smeared) scattering intensity for 2 wt % blends of the various diblocks with the PI homopolymer at the temperature of the interfacial tension measurements (140 °C) as a function of the scattering vector **q**. It is noted that the scattering from homopolymer PI at the same conditions and at the same temperature has been subtracted from the data of the blends in order to subtract the contribution of density fluctuations. Thus, the scattering in Figure 5 corresponds only to concentration fluctuations. It is evident that the scattering intensity is very low for the diblocks with low MW whereas it significantly increases (with a pronounced q dependence) for high MW's. The scattering intensity

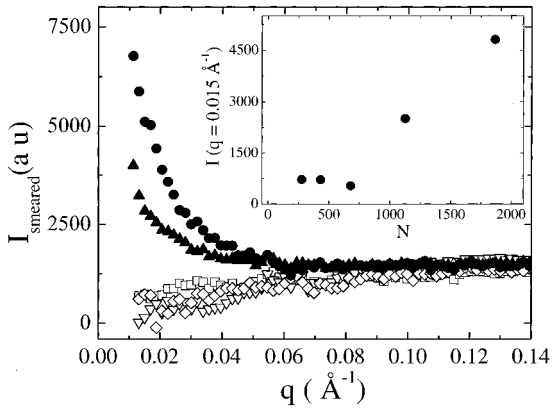

Figure 5. Smeared small-angle X-ray scattering intensity (in arbitrary units) for 2 wt % blends of the various diblocks with the polyisoprene homopolymer at 140 °C as a function of the scattering vector q: (◇) D-2, (□) D-3, (▽) D-4, (▲) D-5, and (●) D-8. The inset shows the scattering intensity at $q = 0.015$ Å^{-1} as a function of N.

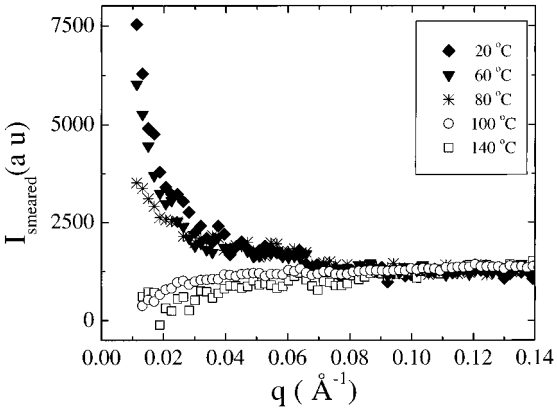

Figure 6. Smeared small-angle X-ray scattering intensity (in arbitrary units) for a 2 wt % D-2/polyisoprene mixture a function of the scattering vector q at various temperature: (◆) 20, (▼) 60, (∗) 80, (○) 100, and (□) 140 °C.

does not increase continuously with the additive MW (which could be attributed to enhanced concentration fluctuations in a homogeneous system by increasing MW), but it essentially jumps from almost negligible values at low N's to high values at higher N's; this is shown in the inset of Figure 5 where the scattering intensity $I_{smeared}$ at a wave vector $q = 0.015$ Å^{-1} is shown as a function of N. Similarly to the analysis of the intensity vs concentration data (at a constant temperature) used[48] to identify the critical micelle concentration, the dependence of $I_{smeared}$ on N signifies the presence of micelles in the blends with the high-N diblocks and their absence for low N's.

However, even for the low MW systems, micelles are evidenced when the temperature is reduced. Figure 6 shows the (smeared) scattering intensity for 2 wt % D-2/PI mixture a function of the scattering vector at various temperatures. The very low intensities for temperatures above 100 °C signify the absence of micelles whereas the high intensities for temperatures below 60 °C are consistent with the micellar formation. The data at 80 °C indicate the so-called "dissolution" of the micelles.[48] Similar behavior is observed for the other systems with low MW's, whereas the blends with the high-MW diblocks do not show the dissolution of micelles at temperatures up to the 140 °C of the interfacial tension measurements. It is noted that, due to the scattering

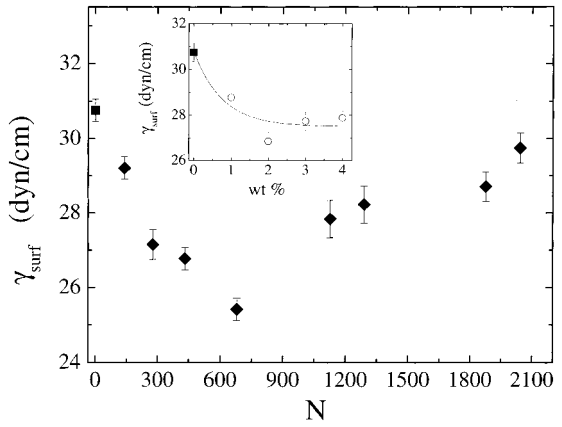

Figure 7. Surface tension for the PS/SI blends in air as a function of number of segments of the copolymers at a constant temperature of 140 ± 1 °C and constant 2 wt % copolymer added. The inset shows the surface tension for the PS/D-5 blends in air as a function of copolymer concentration at a constant temperature of 140 °C with the line being a fit to eq 4 with $\gamma_{surf,sat}$ = 27.4 dyn/cm and $w_{surf,char}$ = 0.76 wt %. ■ denotes the PS surface tension in the absence of the diblock.

vector range of our SAXS camera relative to the apparent size of the micelles, it was not possible to determine neither the size of the micelles not the forward intensity at $q = 0$, which, in principle, can be estimated either from the linear regime of a Guinier plot (ln $I_{smeared}$ vs q^2) or from the linear regime of a Zimm plot ($I_{smeared}^{-1}$ vs q^2). In the accessible q range of the present experiments neither of these plots resulted in a linear regime. However, the intensity data (Figure 5) are sufficient to answer the question posed on the existence or not of micelles in these mixtures.

The SAXS measurements above were performed on homopolymer/copolymer (PI/SI) mixtures. Two points have to be addressed. First, for the interfacial tension measurements, the diblocks were first preblended with PS and this mixture was used vs PI. The symmetry of the diblocks used, however, allows the discussion of the present SAXS data vs the behavior of the interfacial tension; this is supported by the fact that the interfacial tension is essentially unchanged when the additive was preblended with PI or half-and-half with the two homopolymers (Figure 3). Second, the interfacial tension data are for a homopolymer/copolymer/homopolymer (PS/SI/PI) three-component system. Therefore, the possibility for micelle formation should have been investigated for the three-component blend. However, the SAXS scattering in that case would be dominated by the macrophase-separated morphology whereas the contribution to the intensity due to the presence of micelles in either macrophase would be minimal; small-angle neutron scattering experiments on suitable systems with contrast variation are planned to probe the actual situation.

If indeed the micelle formation is the reason for the nonmonotonic dependence of interfacial tension reduction on MW, then it would be more appropriate to compare the SAXS data with the behavior of the polymer/air surface tension of homopolymer/copolymer mixtures, where the presence of micelles should influence the behavior in a similar way. Figure 7 shows the surface tension of the 2 wt % PS/SI mixtures as a function of the copolymer MW at 140 °C. The polymer/air surface tensions were measured with the pendant drop method as described in the Experimental Section with the drop of the PS/SI mixture formed in air. The concentration dependence of the surface tension (shown in the inset of Figure 7 for D-5) demonstrates the surfactant behavior of the SI diblocks as additives in PS. The lower surface tension of the PI block is known to lead to an enrichment[49,57] of the diblock at the PS/air surface thus reducing the surface tension from the value for pure PS, $\gamma_{surf,0} = 30.8 \pm 0.3$ dyn/cm. As the SI concentration increases the surface tension attains a saturation value, $\gamma_{surf,sat}$. Once more, however, this reduction of the surface tension is a nonmonotonic function of the diblock molecular weight: $\Delta\gamma_{surf} = \gamma_{surf,0} - \gamma_{surf,sat}$ first increases with increasing N (for low N's) and then it decreases again with further increase of N. This nonmonotonic behavior is directly related to the SAXS data discussed above. It is noted that the best surfactant behavior for the polymer/polymer interface is observed for diblock D-5 whereas for the polymer/air interface is obtained for diblock D-4. This is due to the different contributions to the free energy associated with a SI chain at the PS/PI interface vs that at a PS/air interface. Actually, it is interesting that the SAXS data for D-5 (Figure 5) show measurable scattering intensity corresponding to the presence of micelles near dissolution; the surface tension data (Figure 7) are consistent with D-5 being in the "high"-MW regime.

IV. Concluding Remarks

The emulsifying effect of symmetric diblock copolymers additives on the interfacial tension between two immiscible homopolymers was investigated using the pendant drop technique. The effects of the concentration and the MW of the additive were studied. The observed dependence of the interfacial tension on the additive concentration agrees with previous investigations: a sharp decrease with addition of a small amount of copolymer followed by a leveling off at higher copolymer concentrations. The dependence of the interfacial tension reduction on the copolymer MW, however, was found to be a nonmonotonic function at constant copolymer concentration. The emulsifying effect, $\Delta\gamma = \gamma_0 - \gamma$ at the plateau region, increases by increasing the additive MW for low MW's whereas it decreases by further increasing the copolymer MW, thus going through a maximum. This is understood by considering the possibility of micelle formation as the additive MW increases leading to a three state equilibrium among copolymer chains adsorbed at the interface, chains homogeneously mixed in the bulk phases and copolymers at micelles within the bulk phases. A model suggested shows the same qualitative behavior but fails to quantitatively account for the effect due to assumptions involved in the estimation of the free energies of the various chain conformations. The presence of micelles for high additive MW's and their absence for low MW's (at the temperature of the interfacial tension measurements) is supported by small-angle X-ray scattering data.

It is important to note that the concentration dependence of the surface tension in solvent/additive systems is traditionally used for the estimation of the critical micelle concentration (cmc) in either small-molecule[61] or polymeric[62−65] surfactant solutions. In those measurements,[63−65] the surface tension decreases with increasing concentration for concentrations up to a certain value and then attains an almost constant value; the break in the γ_{surf} vs log c (c is the additive concentration)

curve is used to denote the cmc. In the present study, however, it is found that even for concentrations in the plateau region (higher than the break) in the interfacial tension (or surface tension) vs concentration curve, micelles are not present for low additive MW's whereas they are present only for higher MW's. Therefore, it is apparent that the break in the interfacial tension vs concentration curve should denote interfacial saturation and not necessary micellization. This is also supported by an early study[66] of polystyrene-*block*-poly(hexyl methyl siloxane)-*block*-polystyrene triblock copolymer solutions in benzene, where although the surface tension data exhibited the break discussed above, no micellization was established by static light scattering; no aggregation was expected since benzene is a good solvent for the blocks. Note that light scattering is one of the methods employed for the investigation of micellization, where the concentration dependence of the light scattering intensity shows a significant change of slope when micelles are formed.[67] The situation when both surface segregation (adsorption at a solid surface) and micellization may occur was investigated theoretically[68] where it was found that depending on the incompatibility of the surface active block with the (monomeric or polymeric) solvent and its (attractive) interactions with the surface, one may have either only adsorption onto the surface or only micellization or an equilibrium of chains adsorbed onto the surface and chains in a micelle. This competition is currently under investigation in copolymer/solvent systems.

Acknowledgment. We thank N. Hadjichristidis, H. Watanabe, K. Adachi, J. W. Mays, M. Pitsikalis, S. Pispas, and K. Hong for kindly supplying the diblock copolymers used in the present study. We thank K. R. Shull for useful discussions. We would like to acknowledge that part of this research was sponsored by NATO's Scientific Affairs Division in the frameworks of the Science for Stability and Science for Peace Programs and by the Greek General Secretariat of Research and Technology (PENED Program).

References and Notes

(1) *Polymer Blends*; Paul, D. R.; Newman, S., Eds.; Academic Press: New York, 1978. Olabisi, O.; Robeson, L. M.; Shaw, M. T. *Polymer−Polymer Miscibility;* Academic Press: New York, 1979. *Polymer Blends Set: Formulation and Performance*; Paul, D. R., Bucknall, C. B., Eds.; John Wiley & Sons: New York, 2000.

(2) Fayt, R.; Jérôme, R.; Teyssié, Ph. *J. Polym. Sci., Polym. Lett.* **1986**, *24*, 25. Fayt, R.; Jérôme, R.; Teyssié, Ph. In *Polyblends—'86*; Utracki, L. A., Ed.; NRCC/IMRI Polymers Symposium Series; IMRA: Montreal, Canada, 1986.

(3) Shull, K. R.; Kramer, E. J.; Hadziioannou, G.; Tang, W. *Macromolecules* **1990**, *23*, 4780. Dai, K. H.; Kramer, E. J.; Shull, K. R. *Macromolecules* **1992**, *25*, 220. Dai, K. H.; Kramer, E. J. *J. Polym. Sci., Part B: Polym. Phys.* **1994**, *32*, 1943.

(4) Green, P. F.; Russell, T. P. *Macromolecules* **1991**, *24*, 2931.

(5) Dai, K. H.; Washiyama, J.; Kramer, E. J. *Macromolecules* **1994**, *27*, 4544.

(6) Russell, T. P.; Anastasiadis, S. H.; Menelle, A.; Felcher, G.; Satija, S. K. *Macromolecules* **1991**, *24*, 1575.

(7) Russell, T. P.; Mayes, A. M.; Deline, V. R.; Chung, T. C. *Macromolecules* **1992**, *25*, 5783. Dai, K. H.; Norton, L. J.; Kramer, E. J. *Macromolecules* **1994**, *27*, 1949.

(8) Patterson, H. T.; Hu, K. H.; Grindstaff, T. H. *J. Polym. Sci., Part C* **1971**, *34*, 31. Gailard, P.; Ossenbach-Sauter, M.; Riess, G. *Makromol. Chem., Rapid Commun.* **1980**, *1*, 771. Gailard, P.; Ossenbach-Sauter, M.; Riess, G. In *Polymer Compatibility and Incompatibility: Principles and Practice*; Solc, K., Ed.; MMI Symposium Series 2; Harwood: New York, 1982; p 289.

(9) Anastasiadis, S. H. Ph.D. Dissertation, Princeton University, Princeton, NJ, 1988.

(10) Anastasiadis, S. H.; Gancarz, I.; Koberstein, J. T. *Macromolecules* **1989**, *22*, 1449.

(11) Wagner, M.; Wolf, B. A. *Polymer* **1993**, *34*, 1461. Jorzik, U.; Wolf, B. A. *Macromolecules* **1997**, *30*, 4713.

(12) Hu, W.; Koberstein, J. T.; Lingelser, J. P.; Gallot, Y. *Macromolecules* **1995**, *28*, 5209. Cho, D.; Hu, W.; Koberstein, J. T.; Lingelser, J. P.; Gallot, Y. *Macromolecules* **2000**, *33*, 5245.

(13) Heikens, D.; Barentsen, W. M. *Polymer* **1977**, *18*, 70.

(14) Fayt, R.; Jérôme, R.; Teyssié, Ph. *J. Polym. Sci., Polym. Lett.* **1981**, *19*, 79. Sundararaj, U.; Macosco, C. W. *Macromolecules* **1995**, *28*, 2647. Macosco, C. W.; Guegan, P.; Khandpur, A.; Nakayama, A.; Marechal, P.; Inoue, T. *Macromolecules* **1996**, *29*, 5590.

(15) Thomas, S.; Prud'homme, R. E. *Polymer* **1992**, *33*, 4260.

(16) Tang, T.; Huang, B. *Polymer* **1994**, *35*, 281.

(17) Brown, H. *Macromolecules* **1989**, *22*, 2859. Brown, H. *Annu. Rev. Mater. Sci.* **1991**, *21*, 463. Creton, C.; Kramer, E. J.; Hadziioannou, G. *Macromolecules* **1991**, *24*, 1846. Washiyama, J.; Kramer, E. J.; Hui, C.-Y. *Macromolecules* **1993**, *26*, 2928. Brown, H.; Char, K.; Deline, V. R.; Green, P. F. *Macromolecules* **1993**, *26*, 4155. Char, K.; Brown, H.; Deline, V. R. *Macromolecules* **1993**, *26*, 4164. Dai, C.-A.; Kramer, E. J.; Washiyama, J.; Hui, C.-Y. *Macromolecules* **1996**, *29*, 7536. Dai, C.-A.; Jandt, K. D.; Iyengar, D. R.; Slack, N. L.; Dai, K. H.; Davidson, W. B.; Kramer, E. J.; Hui, C.-Y. *Macromolecules* **1997**, *30*, 549.

(18) Paul, D. R.; Locke, C. E.; Vinson, C. E. *Polym. Eng. Sci.* **1973**, *13*, 202. Fayt, R.; Jérôme, R.; Teyssié, Ph. In *Multiphase Polymers: Blends and Ionomers*; Utracki, L. A., Weiss, R. A., Eds.; ACS Symposium Series 395, American Chemical Society: Washington, DC, 1989; p 38.

(19) Russell, T. P.; Menelle, A.; Hamilton, W. A.; Smith, G. S.; Satija, S. K.; Majkrzak, C. F. *Macromolecules* **1991**, *24*, 5721.

(20) Ramos, A. R.; Cohen, R. E. *Polym. Eng. Sci.* **1977**, *17*, 639. Marie, P.; Selb, J.; Rameau, A.; Duplessix, R.; Gallot, Y. In *Polymer Blends and Mixtures*; Walsh, D. J., Higgins, J. S., Maconnachie, A., Eds.; NATO Advanced Science Institute Series, Mortinus Nijhoff: Dordrecht, The Netherlands, 1985; p 449.

(21) Ouhadi, T.; Fayt, R.; Jérôme, R.; Teyssié, Ph. *Polym. Commun.* **1986**, *27*, 212. Ouhadi, T.; Fayt, R.; Jérôme, R.; Teyssié, Ph. *J. Polym. Sci., Polym. Phys.* **1986**, *24*, 973.

(22) Duke, T. A. J. Ph.D. Dissertation, University of Cambridge, Cambridge, U.K., 1989.

(23) Fischel, L. B.; Theodorou, D. N. *J. Chem. Soc., Faraday Trans.* **1995**, *91*, 2381.

(24) Werner, A.; Schmid, F.; Binder, K.; Muller, M. *Macromolecules* **1996**, *29*, 8241.

(25) Kim, S. H.; Jo, W. H. *J. Chem. Phys.* **1999**, *110*, 12193.

(26) Vilgis, T. A.; Noolandi, J. *Makromol. Chem., Macromol. Symp.* **1988**, *16*, 225; *Macromolecules* **1990**, *23*, 2941.

(27) Balazs, A. C.; Lyatskaya, J.; Gersappe, D. *Macromolecules* **1995**, *28*, 6278. Gersappe, D.; Balazs, A. C. *Phys. Rev. Lett.* **1995**, *52*, 5061. Lyatskaya, J.; Jacobson, S. H.; Balazs, A. C. *Macromolecules* **1996**, *29*, 1059. Lyatskaya, J.; Gersappe, D.; Gross, N. A.; Balazs, A. C. *J. Phys. Chem.* **1996**, *100*, 1449. Dadmun, M. *Macromolecules* **1996**, *29*, 3868. Kulasekere, R.; Kaiser, H.; Ankner, J. F.; Russell, T. P.; Brown, H. R.; Hawker, C. J.; Mayes, A. M. *Macromolecules* **1996**, *29*, 5493. Lyatskaya, J.; Balazs, A. C. *Macromolecules* **1996**, *29*, 7581. Dadmun, M. *Macromolecules* **2000**, *33*, 9122.

(28) Noolandi, J.; Hong, K. M. *Macromolecules* **1982**, *15*, 482; **1984**, *17*, 1531. Noolandi, J. *Polym. Eng. Sci.* **1984**, *24*, 70. Noolandi, J. *Polym. Prepr.* **1987**, *28*, 46. Noolandi, J. *Makromol. Chem. Rapid Commun.* **1991**, *12*, 517.

(29) Leibler, L. *Makromol. Chem., Macromol. Symp.* **1988**, *16*, 1; *Physica A* **1991**, *172*, 258.

(30) Shull, K. R.; Kramer, E. J. *Macromolecules* **1990**, *23*, 4769.

(31) Israels, R.; Jasnow, D.; Balazs, A. C.; Guo, L.; Krausch, G.; Sokolov, J.; Rafailovich, M. *J. Chem. Phys.* **1995**, *102*, 8149.

(32) Whitmore, M. D.; Noolandi, J. *Macromolecules* **1985**, *18*, 657.

(33) Shull, K. R.; Winey, K. I.; Thomas, E. L.; Kramer, E. J. *Macromolecules* **1991**, *24*, 2748.

(34) Semenov, A. N. *Macromolecules* **1992**, *25*, 4967.

(35) Anastasiadis, S. H.; Chen, J.-K.; Koberstein, J. T.; Siegel, A. F.; Sohn, J. E.; Emerson, J. A. *J. Colloid Interface Sci.* **1987**, *119*, 55. Anastasiadis, S. H.; Gancarz, I.; Koberstein, J. T. *Macromolecules* **1988**, *21*, 2980.

(36) Retsos, H.; Anastasiadis, S. H.; Pispas, S.; Hadjichristidis, N.; Mays, J. W.; Watanabe, H. *Macromolecules*, to be submitted.

(37) Karatasos, K.; Anastasiadis, S. H.; Semenov, A. N.; Fytas, G.; Pitsikalis, M.; Hadjichristidis, N. *Macromolecules* **1994**, *27*, 3543.
(38) Watanabe, H. *Macromolecules* **1995**, *28*, 5006. Karatasos, K.; Anastasiadis, S. H.; Pakula, T.; Watanabe, H. *Macromolecules* **2000**, *33*, 523.
(39) Adachi, K. Private communication.
(40) Anastasiadis, S. H.; Chrissopoulou, K.; Fytas, G.; Fleischer, G.; Pispas, S.; Pitsikalis, M.; Mays, J. W.; Hadjichristidis, N. *Macromolecules* **1997**, *30*, 2445.
(41) Mays, J. W.; Hong, K. Private communication.
(42) Anastasiadis, S. H.; Chrissopoulou, K.; Fytas, G.; Appel, M.; Fleischer, G.; Adachi, K.; Gallot, Y. *Acta Polym.* **1996**, *47*, 250.
(43) Xing, P.; Bousmina, M.; Rodrigue, D.; Kamal, M. R. *Macromolecules* **2000**, *33*, 8034.
(44) Bashforth, S.; Adams, J. C. *An Attempt to Test the Theory of Capillary Action*; Cambridge University Press and Deighton, Bell & Co.: London, 1882.
(45) Richardson, M. J.; Savill, N. G. *Polymer* **1977**, *18*, 3.
(46) Han, C. D.; Kim, J.; Kim, J. K. *Macromolecules* **1989**, *22*, 383.
(47) Strobl, G. R. *Acta Crystallogr., Sect. A* **1970**, *A26*, 367.
(48) Rigby, D.; Roe, R.-J. *Macromolecules* **1984**, *17*, 1778; **1986**, *19*, 721. Roe, R.-J. *Macromolecules* **1986**, *19*, 728. Nojima, S.; Roe, R.-J.; Rigby, D.; Han, C. C. *Macromolecules* **1990**, *23*, 4305.
(49) Leibler, L. *Macromolecules* **1982**, *15*, 1283.
(50) Noolandi, J.; Hong, K. M. *Ferroelectrics* **1980**, *30*, 117. Hong, K. M.; Noolandi, J. *Macromolecules* **1981**, *14*, 72.
(51) Noolandi, J. Private communication, 1987.
(52) Kunz, K.; Anastasiadis, S. H.; Stamm, M.; Schurrat, T.; Rauch, F. *Eur. Phys. J. B* **1999**, *7*, 411.
(53) Shull, K. R. *Macromolecules* **1993**, *26*, 2346.
(54) Helfand, E.; Tagami, Y. *J. Chem. Phys.* **1971**, *56*, 3592; **1972**, *57*, 1812.
(55) Shull and Kramer[30] included the contribution due to composition gradients in the adsorbed layer by including in the right-hand-side of eq 6 a term[9, 35b] $b^{-1}\int_{-\infty}^{\infty} dx\,(\partial\phi_c(x)/\partial x)^2[36\phi_c(x)(1-\phi_c(x))]^{-1}$.
(56) de Gennes, P. G. *Macromolecules* **1980**, *13*, 1069.
(57) It is noted that Noolandi[28e] objects to the use of eqs 5 and 9 since he claims that the main contribution to the interfacial tension reduction is of enthalpic and not entropic origin (as eq 9 suggests), i.e. that it is due to the favor energetics of the orientation of the copolymer blocks into their respective homopolymers and that entropic effects are second order. He suggests that eq 9 should be corrected by adding the contributions of the orientational entropy of the blocks and their entropy of localization; the later was introduced by Shull and Kramer[30] by replacing γ_0 by $\gamma_0' = \gamma_0 + \sigma k_B T \ln[(L_A + L_B)/d']$. In the present analysis the Leibler[29,4] expression is utilized.
(58) Semenov, A. N. *Zh. Eksp. Teor. Fiz.* **1985**, *88*, 1242; *Sov. Phys. JETP* **1985**, *61*, 733.
(59) Munch, M. R.; Gast, A. P. *Macromolecules* **1988**, *21*, 1360.
(60) Budkowski, A.; Steiner, U.; Klein, J.; Fetters, L. J. *Europhys. Lett.* **1992**, *20*, 499. Budkowski, A.; Klein, J.; Fetters, L. J. *Macromolecules* **1995**, *28*, 8571.
(61) Adamson, A. W.; Gast, A. P. *Physical Chemistry of Surfaces*, 6th ed.; John Wiley & Sons: New York, 1997.
(62) Piirma, I. *Polymeric Surfactants*; Marcel Dekker: New York, 1992.
(63) Nakamura, K.; Endo, R.; Takada, M. *J. Polym. Sci., Polym. Phys.* **1976**, *14*, 1287.
(64) Gia, H. B.; Jérôme, R.; Teyssié, Ph. *J. Polym. Sci., Polym. Phys.* **1980**, *18*, 2391.
(65) Riess, G.; Rogez, D. *Polym. Prepr.* **1982**, *23*, 19. Wilson, D. J.; Hurtrez, G.; Riess, G. In *Polymer Blends and Mixtures*; Walsh, D. J., Higgins, J. S., Maconnachie, A., Eds.; NATO Advanced Science Institute Series; Mortinus Nijhoff: Dordrecht, The Netherlands, 1985; p 195.
(66) Owen, M. J.; Kendrick, T. C. *Macromolecules* **1970**, *3*, 458.
(67) Tuzar, Z.; Kratochvil, P. *Makromol. Chem.* **1972**, *160*, 301; *Adv. Colloid Interface Sci.* **1976**, *6*, 201.
(68) Munch, M. R.; Gast, A. P. *Macromolecules* **1988**, *21*, 1366.

MA002105S